

A new $Mn_4^{II}Mn_4^{III}$ cluster from the use of methyl 2-pyridyl ketone oxime in manganese carboxylate chemistry: Synthetic, structural and magnetic studies

Constantinos C. Stoumpos^a, Theocharis C. Stamatatos^b, Vassilis Psycharis^c, Catherine P. Raptopoulou^c, George Christou^{b,*}, Spyros P. Perlepes^{a,*}

^a Department of Chemistry, University of Patras, GR-265 04 Patras, Greece

^b Department of Chemistry, University of Florida, Gainesville, FL 32611-7200, USA

^c Institute of Materials Science, NCSR "Demokritos", GR-153 10 Aghia Paraskevi Attikis, Greece

ARTICLE INFO

Article history:

Received 26 July 2008

Accepted 13 September 2008

Available online 24 October 2008

Keywords:

Crystal structures

Magnetochemistry

Manganese benzoate chemistry

Methyl 2-pyridyl ketone oxime metal

complexes

Mixed-valent manganese clusters

ABSTRACT

The use of methyl 2-pyridyl ketone oxime (mpkoH) in manganese benzoate chemistry is reported. The reaction of $Mn(O_2CPh)_2 \cdot 2H_2O$ with two equivalents of mpkoH in CH_2Cl_2 affords the mononuclear complex $[Mn^{II}(O_2CPh)_2(mpkoH)_2]$ (**2**) in high yield. The Mn^{II} atom is coordinated by two monodentate $PhCO_2^-$ groups and two *N,N'*-bidentate mpkoH chelates in a *cis-cis-trans* fashion. Reaction mixtures comprising $(NBu^4)_4[Mn_4^{III}O_2(O_2CPh)_9(H_2O)]$ and mpkoH in CH_2Cl_2 , $[Mn^{II}Mn^{III}O(O_2CPh)_6(py)_2(H_2O)]$ and mpkoH in CH_2Cl_2 , or $Mn(O_2CPh)_2 \cdot 2H_2O$, $NBu^4 MnO_4$ and mpkoH in $MeOH/MeCN/CH_2Cl_2$ all lead to the mixed-valent cluster $[Mn_4^{II}Mn_4^{III}O_2(OH)_2(O_2CPh)_{10}(mpko)_4]$ (**3**) in moderate yields. The cluster molecule has the $[Mn_8(\mu_4-O)_2(\mu_3-OH)_2]^{14+}$ core (another description of the core is $[Mn_8(\mu_4-O)_2(\mu_3-OH)_2(\mu-OR'')_4(\mu-ONR''')_4]^{6+}$). Peripheral ligation is provided by two η^1 , four $\eta^1:\eta^1:\mu$ and four $\eta^1:\eta^2:\mu_3$ $PhCO_2^-$ groups, as well as four $\eta^1:\eta^1:\eta^1:\mu$ mpko⁻ ligands. Variable-temperature, solid-state dc and ac magnetic studies were carried out on complex **3** in the 5.0–300 K (dc) and 1.8–10 K (ac) ranges. The data reveal dominant antiferromagnetic interactions and a resulting $S = 0$ ground state, which is rationalized in terms of the strong antiferromagnetic coupling within the central $\{Mn_2^{III}O_2\}^{2+}$ subunit.

© 2008 Elsevier Ltd. All rights reserved.

1. Introduction

The last two decades have witnessed a tremendous growth in the interest in polynuclear manganese carboxylate compounds (clusters) with oxygen- and nitrogen-based ligation. This has been mainly due to their relevance to two fields, bioinorganic chemistry and molecular magnetism, as well as to the architectural beauty and aesthetically pleasing structures they possess. Mn ions and biological carboxylate ligands are found at the active sites of several redox enzymes, the most fascinating of which is the water-oxidizing complex (WOC) on the donor side of photosystem II in green plants and cyanobacteria [1]; thus, bioinorganic chemists have been trying to recreate with synthetic models the structure, spectroscopic properties and/or function of the active sites of such enzymes [2], and especially so of the $\{Mn_4CaO_x\}$ cluster unit that is present in the WOC. In the molecular magnetism arena, Mn carboxylate clusters containing Mn^{III} have been found to often have large ground state spin (S) values, which combined with a large and negative magnetoanisotropy (as reflected in a large and nega-

tive zero-field splitting parameter, D) have led to some of these complexes being able to function as single-molecule magnets (SMMs) [3]. SMMs are individual molecules or ions that behave as nanoscale magnets below a certain ("blocking") temperature, and thus represent a molecular, 'bottom-up' approach to nanomagnetism. Scientists around the world are currently seeking to raise the blocking temperature in SMMs and extend this phenomenon as far as possible [4].

For the above and other reasons, there continues to be a great need for new synthetic methods [5] and reaction systems (with suitable organic ligands) to new examples of Mn carboxylate clusters. With this in mind, we have been exploring reactions of 2-pyridyl oximes (Fig. 1) with various Mn carboxylate sources [6–11]. There is currently a renewed interest in the coordination chemistry of oximes, with the efforts of several research groups being driven by a number of considerations [12]. 2-Pyridyl oximes [13] are a subclass of oximes whose anions are versatile ligands for a variety of research objectives (including μ_2 and μ_3 behaviour) and have been central players in several areas of molecular magnetism including single-molecule and single-chain magnetism [12c,13,14]. We recently reported, for example, the employment of mpkoH in Mn carboxylate chemistry, which gave the initial examples of triangular Mn^{III} SMMs by switching the exchange coupling from the more usual antiferromagnetic to ferromagnetic

* Corresponding authors. Tel.: +1 352 392 6737; fax: +1 352 392 8757 (G. Christou); tel.: +30 2610 997146; fax: +30 2610 997118 (S.P. Perlepes).

E-mail addresses: christou@chem.ufl.edu (G. Christou), perlepes@patras.upatras.gr (S.P. Perlepes).

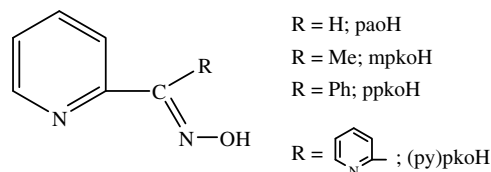


Fig. 1. General structural formula and abbreviations of the 2-pyridyl oximes that are used in our laboratories, including methyl 2-pyridyl ketone oxime (mpkoH) employed in this work.

[9–11]. As an extension to this work, we have now asked if other products might result from the $\text{Mn}/\text{R}'\text{CO}_2^-/\text{mpkoH}$ reaction system. Four years ago, we described in detail the synthesis and structural, spectroscopic and magnetochemical characterization of the remarkable cluster $[\text{Mn}_2^{\text{II}}\text{Mn}_4^{\text{III}}\text{O}_2(\text{OH})_2(\text{O}_2\text{CPh})_{10}(\text{ppko})_4]$ (**1**) and showed that it has a $S = 0$ ground state [7]. We have wondered if the mpko^- analogue of **1** could be prepared and have thus pursued its synthesis. There are two reasons to prepare such a complex: (i) to determine if it would be isostructural with **1** and be isolated at the same oxidation level, and (ii) if it is isostructural, to assess any influence of the Me versus Ph difference on magnetochemical properties. We herein report the successful development of synthetic procedures to prepare the mpko^- analogue of **1** and describe its characterization.

2. Experimental

2.1. General and physical measurements

All manipulations were performed under aerobic conditions using materials (reagent grade) and solvents as received. $\text{Mn}(\text{O}_2\text{CPh})_2 \cdot 2\text{H}_2\text{O}$ [15a], $\text{NBU}^n_4\text{MnO}_4$ [15b], $(\text{NBU}^n_4)[\text{Mn}^{\text{III}}_4\text{O}_2(\text{O}_2\text{CPh})_9(\text{H}_2\text{O})]$ [15a] and $[\text{Mn}_3\text{O}(\text{O}_2\text{CPh})_6(\text{py})_2(\text{H}_2\text{O})]$ [16] were synthesized according to published methods. Elemental analyses (C, H, N) were performed by the in-house facilities of the University of Florida Chemistry Department. IR spectra ($4000\text{--}400\text{ cm}^{-1}$) were recorded on Perkin-Elmer 16 PC and Nicolet Nexus 670 FTIR spectrometers with samples prepared as KBr pellets. Variable-temperature dc and ac magnetic susceptibility data were collected at the University of Florida using a Quantum Design MPMS-XL SQUID susceptometer equipped with a 7 T magnet. The sample was embedded in eicosane to prevent torquing. Diamagnetic corrections were applied to the observed paramagnetic susceptibilities using Pascal's constants.

2.2. Compound preparation

2.2.1. $[\text{Mn}(\text{O}_2\text{CPh})_2(\text{mpkoH})_2]$ (**2**)

Solid mpkoH (0.082 g, 0.60 mmol) was added to a pale pink solution of $\text{Mn}(\text{O}_2\text{CPh})_2 \cdot 2\text{H}_2\text{O}$ (0.100 g, 0.30 mmol) in CH_2Cl_2 (30 mL). The solid soon dissolved to give a yellow solution. The solution was stirred for 30 min and layered with $\text{Et}_2\text{O}/n\text{-hexane}$ (1:1 v/v, 60 mL). After 1 d, X-ray quality, yellow prismatic crystals of the product were collected by filtration, washed with Et_2O ($2 \times 2\text{ mL}$), and dried in air. Yield: 85%. *Anal.* Calc. for $\text{C}_{28}\text{H}_{26}\text{MnN}_4\text{O}_6$: C, 59.05; H, 4.61; N, 9.84. Found: C, 58.97; H, 4.32; N, 9.72%. IR (KBr, cm^{-1}): $\sim 3488\text{mb}$, 3065w, 1599s, 1543s, 1478m, 1437m, 1404s, 1327m, 1255w, 1170w, 1137w, 1098w, 1047s, 1024m, 964w, 834w, 786s, 720s, 684m, 674s, 636w, 563w, 452m, 406w.

2.2.2. $[\text{Mn}_8\text{O}_2(\text{OH})_2(\text{O}_2\text{CPh})_{10}(\text{mpko})_4]$ (**3**)

2.2.2.1. Method A. To a deep red solution of $(\text{NBU}^n_4)[\text{Mn}_4^{\text{III}}\text{O}_2(\text{O}_2\text{CPh})_9(\text{H}_2\text{O})]$ (0.160 g, 0.10 mmol) in CH_2Cl_2 (30 mL) was

added solid mpkoH (0.054 g, 0.40 mmol). The resulting dark brown solution was stirred for 30 min, during which time no further colour change occurred. The solution was filtered and the filtrate layered with $\text{Et}_2\text{O}/n\text{-hexane}$ (1:1 v/v, 60 mL). After 2 d, dark red prismatic crystals of $\mathbf{3} \cdot 1.8\text{CH}_2\text{Cl}_2 \cdot 1.8\text{Et}_2\text{O}$ were collected by filtration, washed with cold Et_2O ($2 \times 2\text{ mL}$), and dried in air. Yield: 60%. The air-dried sample analyzed as $\mathbf{3} \cdot 2\text{H}_2\text{O}$. *Anal.* Calc. for $\text{C}_{98}\text{H}_{84}\text{Mn}_8\text{N}_8\text{O}_{30}$: C, 51.32; H, 3.70; N, 4.88. Found: C, 51.51; H, 3.84; N, 4.83%. IR (KBr, cm^{-1}): 3435mb, 3063w, 2921w, 1597s, 1553s, 1491w, 1484w, 1447m, 1404s, 1317w, 1273w, 1175w, 1151w, 1098w, 1068m, 1046m, 1025m, 934w, 820w, 778m, 718s, 689w, 676m, 639w, 604m, 537w, 457w.

2.2.2.2. Method B. Treatment of a stirred, dark brown solution of $[\text{Mn}_3\text{O}(\text{O}_2\text{CPh})_6(\text{py})_2(\text{H}_2\text{O})]$ (0.108 g, 0.10 mmol) in CH_2Cl_2 (30 mL) with solid mpkoH (0.027 g, 0.20 mmol) gave a solution of essentially the same colour. This was stirred for 30 min and layered with Et_2O (60 mL). Slow mixing gave dark red prismatic crystals which were collected by filtration, washed with Et_2O ($2 \times 3\text{ mL}$) and dried in air. Yield: 40%. The IR spectrum of the product was identical with that of the authentic material prepared by Method A.

2.2.2.3. Method C. Treatment of a stirred, pale pink solution of $\text{Mn}(\text{O}_2\text{CPh})_2 \cdot 2\text{H}_2\text{O}$ (0.100 g, 0.30 mmol) in MeOH/MeCN (15 mL, 1:2 v/v) with solid $\text{NBU}^n_4\text{MnO}_4$ (0.040 g, 0.12 mmol) resulted in a dark brown solution. Solid mpkoH (0.040 g, 0.29 mmol) was slowly added to the solution, and it soon dissolved to give a somewhat darker solution that was stirred for a further 20 min. The solvents were then evaporated under reduced pressure. The dark brown residue was dissolved in CH_2Cl_2 (30 mL), filtered and the essentially black filtrate layered with Et_2O (60 mL). Slow mixing gave dark red crystals of the product after 4 d, which were collected by filtration, washed with cold CH_2Cl_2 ($2 \times 2\text{ mL}$) and Et_2O (5 mL), and dried in air. Yield: $\sim 35\%$. The IR spectrum of the product was identical with the spectra of the material from Methods A and B. The purity of the sample prepared from this method was also confirmed by microanalytical data.

2.3. Single-crystal X-ray crystallography

The crystallographic data and structure refinement details for the two complexes are summarized in Table 1. A selected crystal of **2** ($0.07 \times 0.35 \times 0.66\text{ mm}$) was mounted in air. Diffraction measurements were made on a Crystal Logic Dual Goniometer diffractometer using graphite-monochromated Mo radiation. Unit cell dimensions were determined and refined by using the angular settings of 25 automatically centered reflections in the range $11^\circ < 2\theta < 23^\circ$. Intensity data were recorded using a θ - 2θ scan to a maximum 2θ value of 50° . Three standard reflections monitored every 97 reflections showed less than 3% variation and no decay. Lorentz, polarization corrections were applied using CRYSTAL LOGIC software. The structure was solved by direct methods using SHELXS-97 [17a] and refined on F^2 by full-matrix least squares techniques with SHELXL-97 [17b]. All H atoms were located by Fourier difference maps and refined isotropically. All non-H atoms were refined anisotropically.

A selected crystal of $\mathbf{3} \cdot 1.8\text{CH}_2\text{Cl}_2 \cdot 1.8\text{Et}_2\text{O}$ ($0.28 \times 0.30 \times 0.55\text{ mm}$), prepared by Method A, was taken from the mother liquor, mounted, and immediately cooled to 103(2) K. Data were collected on a Rigaku R-AXIS SPIDER Image Plate diffractometer using graphite-monochromated Mo radiation. Data collection (ω -scans) to a maximum 2θ value of 51° and processing (cell refinement, data reduction and empirical absorption correction) were performed using the CRYSTALCLEAR program package [17c]. The structure was solved by direct methods using SHELXS-97 [17a] and

Table 1
Crystallographic data for complexes **2** and **3** · 1.8CH₂Cl₂ · 1.8Et₂O

Parameter	2	3 · 1.8CH ₂ Cl ₂ · 1.8Et ₂ O
Formula	C ₂₈ H ₂₆ MnN ₄ O ₆	C ₁₀₇ H _{101.60} Mn ₈ N ₈ O _{29.80} Cl _{3.60}
Formula weight	569.47	2543.50
Crystal system	triclinic	monoclinic
Space group	P $\bar{1}$	C2/c
<i>a</i> (Å)	11.013(4)	31.320(4)
<i>b</i> (Å)	11.608(5)	15.565(2)
<i>c</i> (Å)	11.265(5)	24.495(3)
α (°)	97.50(1)	90
β (°)	95.34(1)	109.49(1)
γ (°)	98.19(1)	90
<i>V</i> (Å ³)	1404.1(10)	11257(3)
<i>Z</i>	2	4
ρ_{calc} (g cm ⁻³)	1.347	1.501
Radiation, λ (Å)	Mo K α , 0.71073	Mo K α , 0.71069
Temperature (K)	298	103
μ (mm ⁻¹)	0.517	1.031
Data collected/unique (<i>R</i> _{int})	5270/4954 (0.0137)	40112/10405 (0.0613)
Data with <i>I</i> > 2 σ (<i>I</i>)	4221	8314
<i>R</i> ₁ (<i>I</i> > 2 σ (<i>I</i>)) ^a	0.0390	0.0831
<i>wR</i> ₂ (<i>I</i> > 2 σ (<i>I</i>)) ^b	0.1024	0.1973

$$^a R_1 = \sum(|F_o| - |F_c|) / \sum(|F_o|)$$

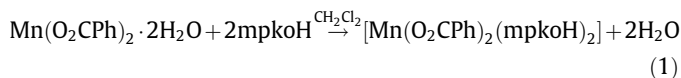
$$^b wR_2 = \{ \sum[w(F_o^2 - F_c^2)^2] / \sum[w(F_o^2)^2] \}^{1/2}$$

refined by full-matrix least squares techniques on *F*² with SHELXL-97 [17b]. All H atoms were introduced at calculated positions and refined as riding on their bound atoms. All non-H atoms were refined anisotropically. Two of the benzoates as well as the solvate molecules were found disordered and refined in two orientations with occupancies adding up to 100%.

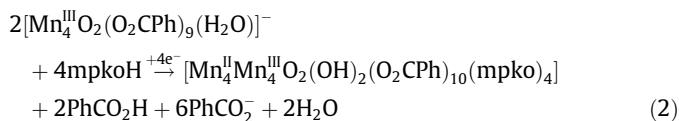
3. Results and discussion

3.1. Syntheses and IR spectroscopy

The preparation of pure **2** in excellent yield was achieved by the reaction of Mn(O₂CPh)₂ · 2H₂O with two equivalents of mpkoH in CH₂Cl₂, see Eq. (1):

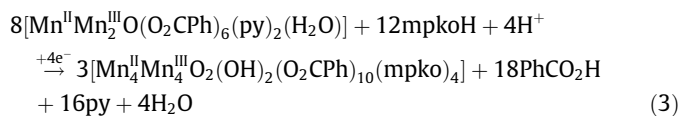


Three procedures to Mn^{II}Mn^{III} complex **3** were developed. The first (and best) involves the conversion of [Mn^{III}O₂(O₂CPh)₉(H₂O)]⁻ into a higher nuclearity product. The anion, which contains only PhCO₂⁻ and H₂O ligands [15a], is a very useful starting material for the synthesis of higher nuclearity clusters [15a,18]. Thus, treatment of the NBU₄⁺ salt of [Mn^{III}O₂(O₂CPh)₉(H₂O)]⁻ with an excess of mpkoH in CH₂Cl₂ led to pure crystalline **3** in good yields (~60%) upon layering of the reaction solution with precipitation solvents. The formation of **3** is summarized in Eq. (2). The 4Mn^{II}, 4Mn^{III} description of **3** requires the reduction of four Mn^{III} ions to have occurred. The source of the reducing agent is probably an



impurity of the solvent or excess ligand groups, facilitated by the strongly oxidizing nature of Mn^{III} [15a]. An alternative means for the generation of the Mn^{II} ions in **3** might be disproportionation of Mn^{III}, in which case Mn^{IV}-containing species would be present in the coloured filtrate [15a]. We have not attempted to identify the exact origin of the Mn^{II} ions in the product, nor would it be a simple investigation.

The second procedure to **3** gave a lower yield and involved the reaction of [Mn^{II}Mn^{III}O(O₂CPh)₆(py)₂(H₂O)] [16] with two equivalents of mpkoH in CH₂Cl₂. Many synthetic procedures to make polynuclear manganese carboxylate clusters rely on the reactions of triangular [Mn₃O(O₂CR)₆L_xL'_y]^{0/+} species (*x* + *y* = 3) with a potentially chelating/bridging ligand [5b,11]. The formation of **3** by this method can be summarized in Eq. (3). As stated above, it is not uncommon to find Mn^{III} – a strong oxidizing agent – being reduced by ligand groups, solvent impurities, etc.:



Once the identity of **3** had been established, we also sought its synthesis from simpler starting materials, and we found that it can be prepared by the comproportionation between Mn(O₂CPh)₂ · 2H₂O and NBU₄⁺MnO₄⁻ [15b] in a 2.5:1 ratio in the presence of mpkoH in MeOH/MeCN. Such comproportionation reactions between Mn^{II} and Mn^{VII} sources in the presence of appropriate ligand groups have found extensive prior use to produce clusters of several nuclearities at various Mn oxidation levels [11,15a,19]. The ratio employed in this work gives, on paper, an average Mn oxidation state in solution of Mn^{+3.4}, higher than that (Mn^{+2.5}) observed in solid **3**, but the MeOH can act as reducing agent. The yield was only ~35%, and it is possible there are other products in the coloured filtrates. We also explored higher Mn^{II}:Mn^{VII} ratios, but this led to **3** contaminated with [Mn^{II}₄Mn^{III}₂O₂(O₂CPh)₁₀(MeCN)₄] [20] containing no bound mpko⁻ groups.

Note that the Mn(O₂CPh)₂ · 2H₂O/MnO₄⁻/mpkoH and [Mn₃O(O₂CPh)₆(py)₂(H₂O)]/mpkoH reaction systems in EtOH or MeOH/MeCN/CH₂Cl₂ in the presence of appropriate counterions (e.g. ClO₄⁻) have led to salts of the [Mn₃O(O₂CPh)₃(mpko)₃]⁺ cation, which were amongst the first examples of SMMs with a triangular structure [9,11]. Thus, it is likely, as with many other reactions in higher oxidation state Mn chemistry, that the reaction solution contains a complicated mixture of several species in equilibrium, with factors such as relative solubilities, absence/presence of counterions, lattice energies, crystallization kinetics and others determining the identity of the isolated product [19].

The presence of neutral oxime groups in **2** is manifested by a broad IR band of medium intensity at 3488 cm⁻¹, assigned to $\nu(\text{OH})_{\text{oxime}}$ [6,21]. The IR spectrum of **3** exhibits a medium band at 3435 cm⁻¹ assignable [22] to $\nu(\text{OH})_{\text{OH}}$. The broadness and relatively low wavenumber of these bands are both indicative of hydrogen-bonding. A medium-intensity band at 604 cm⁻¹ is present in the spectrum of **3**; this band, which is absent from the spectrum of **2**, is tentatively assigned to a vibration involving a Mn^{III}–O²⁻ stretch [23]. The $\nu(\text{CO}_2)$ bands are difficult to assign in the spectra of **2** and **3** due to the appearance of overlapping carboxylate, phenyl, 2-pyridyl and oxime/oximate stretching vibrations in the 1600–1400 cm⁻¹ region [24] and thus the application of the spectroscopic criterion of Deacon and Phillips [25] is very difficult.

3.2. Description of structures

The molecular structures of complexes **2** and **3** are depicted in Figs. 2 and 3, respectively. Selected interatomic distances and angles are listed in Tables 2 and 3.

Complex **2** crystallizes in the triclinic space group P $\bar{1}$. Its structure consists of well-separated [Mn(O₂CPh)₂(mpkoH)₂] molecules. The Mn^{II} center is coordinated by two monodentate PhCO₂⁻ groups and two *N,N'*-chelating (η^2) mpkoH ligands. The mpkoH donor atoms are the nitrogen atoms of the neutral oxime and the 2-pyridyl groups. The six-coordinate molecule is the *cis-cis-trans* isomer

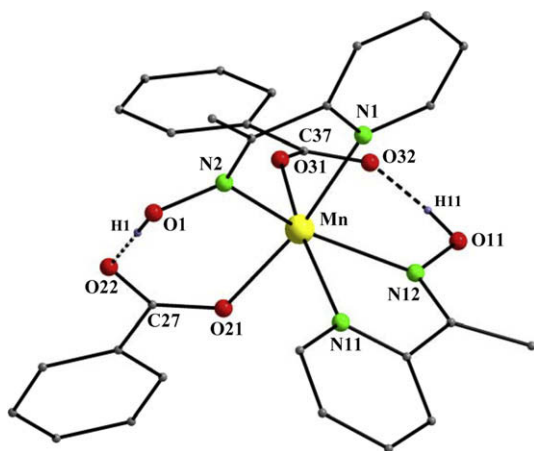


Fig. 2. Partially labelled plot of complex **2**. The dashed lines are H-bonds. Colour scheme: Mn^{II}, yellow; O, red; N, green; C, gray; H, purple. (For interpretation of the references to colour in this figure legend, the reader is referred to the web version of this article.)

with respect to the disposition of the benzoate oxygen, pyridyl nitrogen and oxime nitrogen atoms, respectively. The *cis* arrangement of the oxime groups seems unfavorable, probably due to the steric hindrance arising from the Me groups upon oxime coordination. The molecule has no imposed symmetry, although it closely approximates *C*₂ symmetry, with the pseudo *C*₂ axis bisecting the O(21)–Mn–O(31) angle. The main distortion from octahedral geometry is due to the small bite angles of the mpkoH chelates (70.2°, 70.6°). There are very strong intramolecular H-bonds between unbound oxime –OH groups and the unbound benzoate O atoms (O(22), O(32)). The dimensions are: O(1)···O(21) 2.542(4) Å, HO(1)···O(22) 1.650(4) Å, O(1)–HO(1)···O(22) 178.9(1)° and O(11)···O(32) 2.535 Å, HO(11)···O(32) 1.672(5) Å,

Table 2
Selected bond lengths (Å) and angles (°) for complex **2**

Mn–O(21)	2.104(2)	Mn–N(12)	2.282(2)
Mn–O(31)	2.083(2)	C(27)–O(21)	1.259(3)
Mn–N(1)	2.302(2)	C(27)–O(22)	1.241(4)
Mn–N(2)	2.273(2)	C(37)–O(31)	1.244(3)
Mn–N(11)	2.287(2)	C(37)–O(32)	1.232(3)
O(21)–Mn–O(31)	88.4(1)	O(31)–Mn–N(12)	95.9(1)
O(21)–Mn–N(1)	169.1(1)	N(1)–Mn–N(2)	70.2(1)
O(21)–Mn–N(2)	99.1(1)	N(1)–Mn–N(11)	92.9(1)
O(21)–Mn–N(11)	88.5(1)	N(1)–Mn–N(12)	87.8(1)
O(21)–Mn–N(12)	102.8(1)	N(2)–Mn–N(11)	89.3(1)
O(31)–Mn–N(1)	92.9(1)	N(2)–Mn–N(12)	149.6(1)
O(31)–Mn–N(2)	105.7(1)	N(11)–Mn–N(12)	70.6(1)
O(31)–Mn–N(11)	165.0(1)		

O(11)–HO(11)···O(32) 170.5(1)°. Complex **2** joins a very small family of [Mn^{II}(O₂CR')₂(L–L)₂] complexes (L–L = neutral 2-pyridyl oximes) with an analogous *cis–cis–trans* arrangement of the donor atoms [6–8].

Complex **3** · 1.8CH₂Cl₂ · 1.8Et₂O crystallizes in the monoclinic space group *C*2/*c*. Its structure consists of the [Mn₈O₂(O–H)₂(O₂CPh)₁₀(mpko)₄] molecule and solvate CH₂Cl₂ and Et₂O molecules; the latter will not be further discussed. The molecule lies on a crystallographic twofold axis. The eight Mn ions are held together by two μ₄–O^{2–} (O(71), O(71')) and two μ₃–OH[–] (O(72), O(72')) groups to give a [Mn₈(μ₄–O)₂(μ₃–OH)₂]¹⁴⁺ core (Fig. 4). Bond-valence sum (BVS) calculations [26] give values of 1.8 and 1.2 for O(71) and O(72), respectively, supporting their assignments as oxo and hydroxo oxygen atoms (Table 4). Peripheral ligation is provided by two monodentate (η¹) PhCO₂[–] (those containing the ligating atoms O(51) and O(51')), four *syn,syn*–η¹:η¹:μ PhCO₂[–] (those containing O(41)/O(42), O(61)/O(62) and their symmetry-related partners), four η¹:η²:μ₃ PhCO₂[–] groups (those containing O(21)/O(22), O(31)/O(32') and their symmetry-related partners)

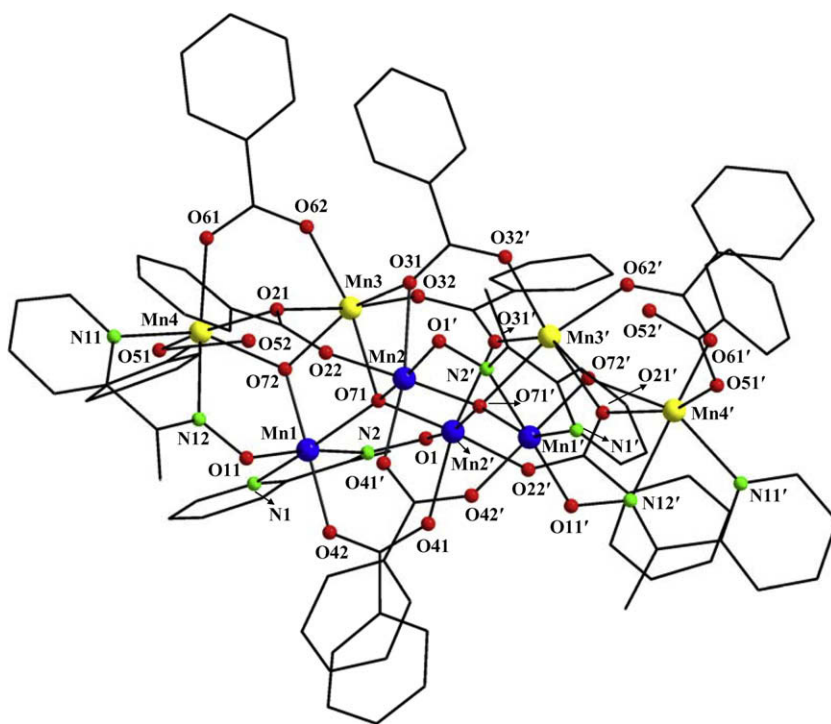


Fig. 3. Partially labelled plot of the Mn₈ molecule of complex **3**. Primed and unprimed atoms are related by the crystallographic two-fold axis. O(71) and O(71') are the oxide ions, and O(72) and O(72') are the hydroxide O atoms. Colour scheme: Mn^{II}, yellow; Mn^{III}, blue; O, red; N, green; C, gray. (For interpretation of the references to colour in this figure legend, the reader is referred to the web version of this article.)

Table 3
Selected interatomic distances (Å) and angles (°) for complex **3** · 1.8CH₂Cl₂ · 1.8Et₂O

Mn(1)···Mn(2)	3.870(6)	Mn(2)–O(31)	2.304(5)
Mn(1)···Mn(3)	3.290(2)	Mn(2)–O(41')	2.173(5)
Mn(1)···Mn(4)	3.531(6)	Mn(2)–O(71)	1.908(4)
Mn(2)···Mn(3)	3.189(1)	Mn(2)–O(71')	1.870(3)
Mn(2)···Mn(4)	5.346(2)	Mn(3)–O(21)	2.238(4)
Mn(3)···Mn(4)	3.365(1)	Mn(3)–O(31)	2.158(4)
Mn(2)···Mn(2')	2.804(2)	Mn(3)–O(32)	2.133(4)
Mn(4)···Mn(4')	10.910(5)	Mn(3)–O(62)	2.131(5)
Mn(1)–O(11)	1.891(4)	Mn(3)–O(71)	2.272(4)
Mn(1)–O(42)	1.954(4)	Mn(3)–O(72)	2.164(4)
Mn(1)–O(71)	2.180(4)	Mn(4)–O(21)	2.450(4)
Mn(1)–O(72)	1.942(4)	Mn(4)–O(51)	2.130(4)
Mn(1)–N(1)	2.273(5)	Mn(4)–O(61)	2.098(5)
Mn(1)–N(2)	2.039(5)	Mn(4)–O(72)	2.163(4)
Mn(2)–O(1')	1.947(4)	Mn(4)–N(11)	2.237(5)
Mn(2)–O(22)	1.978(4)	Mn(4)–N(12)	2.238(6)
O(11)–Mn(1)–N(2)	170.8(2)	O(72)–Mn(4)–N(11)	153.2(2)
O(42)–Mn(1)–O(72)	177.7(2)	Mn(1)–O(71)–Mn(2)	142.3(2)
O(71)–Mn(1)–N(1)	157.2(2)	Mn(1)–O(71)–Mn(2')	107.8(2)
O(1')–Mn(2)–O(71)	167.5(2)	Mn(1)–O(71)–Mn(3)	95.3(2)
O(22)–Mn(2)–O(71')	175.5(2)	Mn(2)–O(71)–Mn(2')	95.8(2)
O(31)–Mn(2)–O(41')	169.5(1)	Mn(2)–O(71)–Mn(3)	99.1(2)
O(21)–Mn(3)–O(32)	173.6(2)	Mn(2')–O(71)–Mn(3)	118.0(2)
O(31)–Mn(3)–O(72)	150.6(2)	Mn(1)–O(72)–Mn(3)	106.4(2)
O(62)–Mn(3)–O(71)	168.8(2)	Mn(1)–O(72)–Mn(4)	118.5(2)
O(21)–Mn(4)–O(51)	161.2(2)	Mn(3)–O(72)–Mn(4)	102.1(2)
O(61)–Mn(4)–N(12)	156.3(2)		

^a Primed atoms are related to the unprimed ones by the symmetry operation $-x, y, -z + 1/2$.

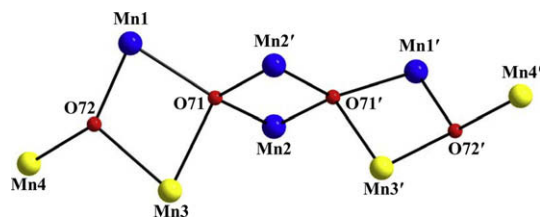


Fig. 4. The $[\text{Mn}_8(\mu_4\text{-O})_2(\mu_3\text{-OH})_2]^{14+}$ core of complex **3**; O(71) and O(71') are the oxide ions, and O(72) and O(72') are the OH⁻ ions. Colour scheme: Mn^{II}, yellow; Mn^{III}, blue; O, red. (For interpretation of the references to colour in this figure legend, the reader is referred to the web version of this article.)

Table 4
Bond valence sum (BVS) calculations^{a,b} for the Mn and selected O atoms in complex **3**

Atom	Mn ^{II}	Mn ^{III}	Mn ^{IV}
Mn(1)	3.17	2.95	3.02
Mn(2)	3.17	2.90	3.05
Mn(3)	1.96	1.79	1.88
Mn(4)	1.98	1.85	1.88
	BVS	Assignment	
O(71)	1.79	O ²⁻	
O(72)	1.17	OH ⁻	

^a The italic value is the one closest to the charge for which it was calculated. The oxidation state of a particular Mn center can be taken as the nearest whole number to the italic value.

^b An O BVS in the ~1.8–2.0, ~1.0–1.2 and ~0.2–0.4 ranges is indicative of zero, single, and double protonation, respectively.

and four $\eta^1:\eta^1:\eta^1:\mu$ mpko⁻ ligands. Each mpko⁻ ligand chelates one metal ion through its nitrogen atoms forming a five-membered ring and bridges this metal ion with a second one through the terminally ligated, deprotonated oximate O atom (O(1), O(1'), O(11), O(11')). If we consider the monoatomic carboxylate bridges and the bridging diatomic oximate groups as part of the core, then the latter becomes $[\text{Mn}_8(\mu_4\text{-O})_2(\mu_3\text{-OH})_2(\mu\text{-OR}')_4(\mu\text{-ONR}''')_4]^{6+}$;

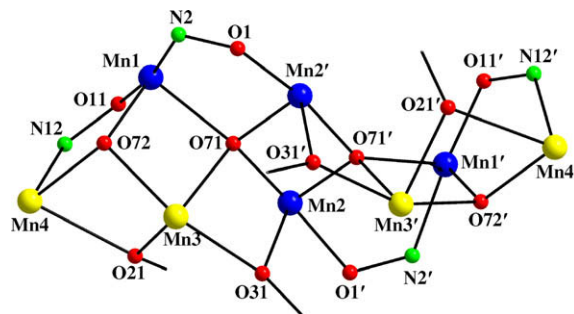


Fig. 5. The core of **3** emphasizing the oxime bridging modes. For the chemical nature of most atoms, see the caption of Fig. 4. O(21), O(31), O(21') and O(31') are the monoatomically bridging benzoate O atoms. N(2), O(1), N(12), and O(11) are the mpko⁻ oximate groups. Colour scheme as in Fig. 3.

this view is emphasized in Fig. 5. The Mn₈ topology of **3** is shown in Fig. 6.

Mn(1) and Mn(4) are bound to an O₄N₂ set of donor atoms, while Mn(2) and Mn(3) to an O₆ set. Charge considerations require a 4Mn^{II}, 4Mn^{III} mixed-valence description, and Mn(1) and Mn(2) are assigned as Mn^{III} on the basis of (i) their shorter average Mn–O bond lengths (2.015 Å) compared with those for Mn(3) and Mn(4) (average 2.194 Å, with no individual value shorter than 2.10 Å); (ii) a Jahn–Teller (JT) axial elongation at Mn(1) and Mn(2) (the JT elongation axes are O(71)–Mn(1)–N(1) and O(31)–Mn(2)–O(41')), as expected for high-spin d⁴ ions in near-octahedral geometry; and (iii) BVS calculations [26] (Table 4). Thus, the hydroxide group bridges one Mn^{III} and two Mn^{II} atoms, while the oxide group bridges one Mn^{II} and three Mn^{III} atoms.

The $\mu\text{-O}$ atom O(21) does not bridge the two Mn^{II} ions symmetrically, with Mn(3)–O(21) (2.238(4) Å) noticeably shorter than Mn(4)–O(21) (2.450(4) Å). The Mn(3,4)–O(72) bond distances (average 2.164(4) Å) are longer than the Mn(1)–O(72) distance (1.942(4) Å), consistent with a higher oxidation state for Mn1. It should also be noted that the O²⁻ groups (O(71), O(71')) bridge the three Mn^{III} atoms in an asymmetric fashion. Thus, Mn(2,2')–O(71) distances average 1.889(4) Å, whereas the Mn(1)–O(1) bond length is noticeably longer (2.180(4) Å). This is the result of O(71) lying on the JT elongation axis of Mn(1); Mn^{III}–O²⁻ distances at ~2.2 Å are extremely rare [27]. The Mn···Mn distances (Table 3) depend on the number and nature of the bridges between two given metal centers and on the oxidation state of each Mn atom. The central Mn(2)···Mn(2') distance is the shortest (2.804(2) Å) and is typical for $\{\text{Mn}_2^{\text{III,III}}(\mu_4\text{-O})_2\}^{2+}$ subunits in Mn^{III}-containing clusters [20,28]. The uncoordinated O atoms of the monodentate PhCO₂⁻ ligands (O(52) and O(52')) are H-bonded to the OH⁻ ligands, with the O(52)···O(72) distance being 2.777(2) Å.

The core of **3** can be described in various ways: (i) as two $\{\text{Mn}_2^{\text{II}}\text{Mn}_2^{\text{III}}(\mu_3\text{-O})(\mu_3\text{-OH})\}^{7+}$ subunits (atoms Mn(1)–Mn(4) and their symmetry equivalents) becoming linked through their $\mu_3\text{-O}$

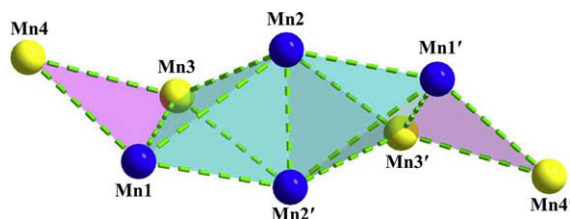


Fig. 6. The Mn₈ skeleton of **3** emphasizing the 'edge-sharing tetrahedra', 'butterfly-like' and various triangular subunits. Colour scheme: Mn^{II}, yellow; Mn^{III}, blue. (For interpretation of the references to colour in this figure legend, the reader is referred to the web version of this article.)

2^- converting to μ_4 and thus providing the two ‘inter-fragment’ Mn(2)–O(71') and Mn(2')–O(71) bonds. The four metal ions in each subunit are nearly coplanar with the Mn(1)–Mn(2)–Mn(3)–Mn(4) torsion angle being 7.18° . The $\{\text{Mn}_2^{\text{II}}\text{Mn}_2^{\text{III}}(\mu_3\text{-O})(\mu_3\text{-OH})\}^{7+}$ subunit has not been seen before in a discrete Mn_4 cluster or as a recognizable sub-fragment of a higher nuclearity cluster; (ii) as a central $\{\text{Mn}_2^{\text{II}}\text{Mn}_4^{\text{III}}(\mu_4\text{-O})\}^{12+}$ subunit (the oxidized version of the familiar $[\text{Mn}_4^{\text{II}}\text{Mn}_2^{\text{III}}(\mu_4\text{-O})_2]^{10+}$ core [29]) with an additional Mn^{II} atom at each end linked through the $\mu_3\text{-OH}^-$ ion. The central $\{\text{Mn}_2^{\text{II}}\text{Mn}_4^{\text{III}}(\mu_4\text{-O})_2\}^{12+}$ subunit consists of six Mn ions arranged as two edge-sharing tetrahedra, each with a central $\mu_4\text{-O}^{2-}$. The Mn– $\mu_4\text{-O}^{2-}$ –Mn angles range from 95.3° to 142.3° , deviating significantly from the 109.5° ideal values of a tetrahedron. The central $\{\text{Mn}_2^{\text{II}}\text{Mn}_4^{\text{III}}(\mu_4\text{-O})_2\}^{12+}$ subunit can also be considered as two $\{\text{Mn}_3\text{O}\}^{6+}$ triangular units (Mn(1,2,3) and Mn(1',2',3')) or, alternatively, Mn(1,2',3) and Mn(1',2,3')) joined together by each of their $\mu_3\text{-O}^{2-}$ ions (O71 and O71') becoming μ_4 by ligating to the Mn^{II} center of the adjacent unit. Note that this central $\{\text{Mn}_6\text{O}_2\}^{12+}$ subunit of **3** is similar to the recently reported Mn_6 cation $[\text{Mn}_2^{\text{II}}\text{Mn}_4^{\text{III}}\text{O}_2(\text{OMe})_2(\text{dapdo})_2(\text{dapdoH})_4]^{12+}$ (dapdoH₂ = 2,6-diacetylpyridine dioxime) [5b]; and (iii) as a central $\{\text{Mn}_4^{\text{III}}(\mu_3\text{-O})_2\}^{8+}$ butterfly-like [15a,30] subunit (atoms Mn(1), Mn(2), Mn(2'), Mn(1'), O(71), O(71')) to which are attached two $\{\text{Mn}_2^{\text{II}}(\mu\text{-OH})\}^{3+}$ subunits via the interfragment bonds Mn(1)–O(72), Mn(3)–O(71) and their symmetry equivalents; as a result, each OH[−] group becomes μ_3 , forming a bond with a ‘wing-tip’ Mn^{III} atom (Mn(1), Mn(1')), and each O^{2-} group is converted to μ_4 forming a bond with one of the Mn^{II} atoms (Mn(3), Mn(3')).

Complex **3** joins only a small family of Mn clusters of nuclearity eight, which currently comprise the metal oxidation levels Mn_8^{II} [31], $\text{Mn}_6^{\text{II}}\text{Mn}_2^{\text{III}}$ [32], $\text{Mn}_4^{\text{II}}\text{Mn}_4^{\text{III}}$ [7,33], $\text{Mn}_2^{\text{II}}\text{Mn}_6^{\text{III}}$ [5b,15a,34], Mn_8^{III} [35] and $\text{Mn}_2^{\text{III}}\text{Mn}_6^{\text{IV}}$ [36], and thus it becomes the fourth member of the $\text{Mn}_4^{\text{II}}\text{Mn}_4^{\text{III}}$ subfamily.

3.3. Magnetochemistry

Variable-temperature dc magnetic susceptibility data in a 0.1 T field and in the 5.0–300 K range were collected on a powdered microcrystalline sample of **3** restrained in eicosane to prevent torquing. The obtained data are plotted as $\chi_{\text{M}}T$ versus T in Fig. 7. The $\chi_{\text{M}}T$ value at 300 K is $29.34 \text{ cm}^3 \text{ K mol}^{-1}$. This value is slightly less than that expected for a cluster comprising four Mn^{II} and four Mn^{III} non-interacting ions ($29.50 \text{ cm}^3 \text{ K mol}^{-1}$ with $g = 2$). The $\chi_{\text{M}}T$ product gradually decreases with decreasing temperature to $15.12 \text{ cm}^3 \text{ K mol}^{-1}$ at 50 K before dropping to $2.99 \text{ cm}^3 \text{ K mol}^{-1}$ at

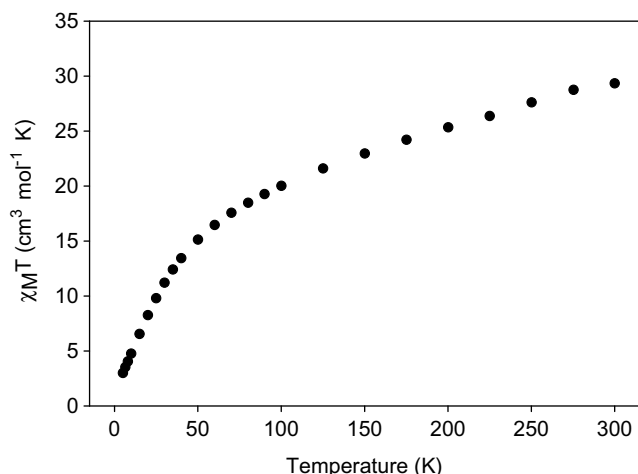


Fig. 7. Plot of $\chi_{\text{M}}T$ vs. T for cluster **3**.

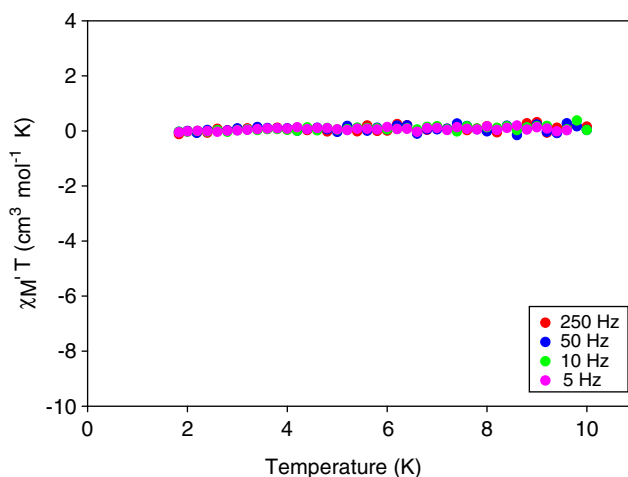


Fig. 8. Plot of the in-phase ac susceptibility signals as a $\chi'_{\text{M}}T$ vs. T plot for complex **3** in a 3.5 G field oscillating at the indicated frequencies.

5.0 K. The $\chi_{\text{M}}T$ versus T data appear to be heading for $0 \text{ cm}^3 \text{ K mol}^{-1}$ at 0 K. This behaviour is indicative of dominant anti-ferromagnetic interactions between the metal centers with the low temperature value suggesting a small ground state spin of $S = 0$ or 1. To determine which one it is, and to avoid complications from an applied dc field, we employed the ac susceptibility technique [37] with a zero dc field and a 3.5 G ac field (Fig. 8). The $\chi'_{\text{M}}T$ signal below 10 K is zero, confirming an $S = 0$ ground state [29], and the essentially constant value in this temperature range indicates little population of excited states.

Similarly low or $S = 0$ ground states have been reported for the other $\text{Mn}_4^{\text{II}}\text{Mn}_4^{\text{III}}$ clusters in the literature [33], and we have provided elsewhere a detailed rationalization of the $S = 0$ ground state for the structurally similar cluster **1** [7] on the basis of the well-established magnetic behaviour of the central, butterfly-like $\{\text{Mn}_4^{\text{III}}(\mu_3\text{-O})_2\}^{8+}$ subcore [30,38].

4. Conclusions

The present work extends the body of results that emphasize the ability of mpkoH to form interesting structural types in Mn carboxylate chemistry. In addition to the $[\text{Mn}_3^{\text{II}}\text{O}(\text{O}_2\text{CR})_3(\text{mpko})_3]^+$ cationic SMMs reported previously [9–11], the Mn/PhCO₂[−]/mpkoH reaction system has provided access to the octanuclear $\text{Mn}_4^{\text{II}}\text{Mn}_4^{\text{III}}$ cluster **3** and the mononuclear Mn^{II} compound **2**. Complex **3** is a new addition to the Mn_8 family of clusters. Although this compound has been found to possess a $S = 0$ spin ground state, the potentially μ_3 mode of mpko[−] (which has not been realized in the present study) [13] would undoubtedly give $\text{Mn}_x/\text{RCO}_2^-/\text{mpko}^-$ products structurally different from **3** and which may have high-spin ground states. The bridging mode(s) of mpko[−] also suggests possibilities for other Mn_x non-carboxylate clusters to exist, e.g. clusters containing the strongly coordinating inorganic anions N_3^- , NCO^- and SO_4^{2-} .

As far as the specific goals of this work mentioned in the Introduction are concerned, it has been demonstrated that the attainment and stability of clusters containing the $[\text{Mn}_4^{\text{II}}\text{Mn}_4^{\text{III}}(\mu_4\text{-O})_2(\mu_3\text{-OH})_2]^{14+}$ core are not limited to the use of ppko[−] (Fig. 1), nor are they in some way a consequence of any specific property of this ligand, other than its chelating/bridging nature. The employment of mpko[−] leads to a product with the same formulation, superimposable cores and almost identical magnetic behaviour. In many ways, this was surprising given how often similarly small changes to a reaction, such as changing the carboxylate or solvent, can lead to a completely different product. There are examples in nickel chemistry

where mpkoH and ppkoH give different products in otherwise similar reactions [24,39]. The presence or absence of counteranions such as ClO_4^- does make a difference, however; its absence from the present reactions precludes formation of the trinuclear $[\text{Mn}_3\text{O}]^{7+}$ -containing, mixed $\text{R}'\text{CO}_2^-/\text{mpko}^-$ complexes, another thermodynamically favorable arrangement and potential product of $\text{Mn}/\text{R}'\text{CO}_2^-/\text{mpko}^-$ components.

Acknowledgements

This work was supported by EPEAEK II (Program PYTHAGORAS I, Grant b.365.037 to S.P.P) and NSF (CHE-0414555 to G.C.).

Appendix A. Supplementary data

CCDC 693825 and 693826 contain supplementary crystallographic data for **2** and **3** · 1.8 CH_2Cl_2 · 1.8 Et_2O . These data can be obtained free of charge via <http://www.ccdc.cam.ac.uk/conts/retrieving.html>, or from the Cambridge Crystallographic Data Centre, 12 Union Road, Cambridge CB2 1EZ, UK; fax: (+44) 1223-336-033; or e-mail: deposit@ccdc.cam.ac.uk. Supplementary data associated with this article can be found, in the online version, at doi:10.1016/j.poly.2008.09.010.

References

- [1] (a) K.N. Ferreira, T.M. Iverson, K. Maghlaoui, J. Barber, S. Iwata, *Science* 303 (2004) 1831; (b) A recent comprehensive review: J. Barber, J.W. Murray, *Coord. Chem. Rev.* 252 (2008) 416.
- [2] (a) A recent review: C.S. Mullins, V.L. Pecoraro, *Coord. Chem. Rev.* 252 (2008) 416; (b) A. Mishra, W. Wernsdorfer, K.A. Abboud, G. Christou, *Chem. Commun.* (2005) 54; (c) I.J. Hewitt, J.K. Tang, N.T. Maddhu, R. Clérac, G. Buth, C.F. Anson, A.K. Powell, *Chem. Commun.* (2006) 2650.
- [3] (a) For reviews see: G. Christou, D. Gatteschi, D.N. Hendrickson, R. Sessoli, *MR Bull.* 25 (2000) 66; (b) D. Gatteschi, R. Sessoli, *Angew. Chem., Int. Ed.* 42 (2003) 268; (c) R. Birchner, G. Chaboussant, C. Dobe, H. Güdel, S.T. Ochsenein, A. Sieber, O. Waldman, *Adv. Funct. Mater.* 16 (2006) 209; (d) G. Aromi, E.K. Brechin, *Struct. Bond.* 122 (2006) 1.
- [4] (a) Th.C. Stamatatos, G. Christou, *Philos. Trans. Roy. Soc. (A)* 366 (2008) 113; (b) C.J. Milios, A. Vinslava, W. Wernsdorfer, S. Moggach, S. Parsons, S.P. Perlepes, G. Christou, E.K. Brechin, *J. Am. Chem. Soc.* 129 (2007) 2754.
- [5] (a) G. Christou, *Polyhedron* 24 (2005) 2065; (b) Th.C. Stamatatos, B.S. Luisi, B. Moulton, G. Christou, *Inorg. Chem.* 47 (2008) 1134, and references cited therein.
- [6] C.J. Milios, E. Keffalloniti, C.P. Raptopoulou, A. Terzis, A. Escuer, R. Vicente, S.P. Perlepes, *Polyhedron* 23 (2004) 83.
- [7] C.J. Milios, Th.C. Stamatatos, P. Kyritsis, A. Terzis, C.P. Raptopoulou, R. Vicente, A. Escuer, S.P. Perlepes, *Eur. J. Inorg. Chem.* (2004) 2885.
- [8] C.J. Milios, P. Kyritsis, C.P. Raptopoulou, A. Terzis, R. Vicente, A. Escuer, S.P. Perlepes, *Dalton Trans.* (2005) 501.
- [9] Th.C. Stamatatos, D. Foguet-Albiol, C.C. Stoumpos, C.P. Raptopoulou, A. Terzis, W. Wernsdorfer, S.P. Perlepes, G. Christou, *Polyhedron* 26 (2007) 2165.
- [10] S.-C. Lee, Th.C. Stamatatos, D. Foguet-Albiol, S. Hill, S.P. Perlepes, G. Christou, *Polyhedron* 26 (2007) 2255.
- [11] Th.C. Stamatatos, D. Foguet-Albiol, S.-C. Lee, C.C. Stoumpos, C.P. Raptopoulou, A. Terzis, W. Wernsdorfer, S.O. Hill, S.P. Perlepes, G. Christou, *J. Am. Chem. Soc.* 129 (2007) 9484.
- [12] (a) For reviews see: V.Yu. Kukushkin, A.J.L. Pombeiro, *Coord. Chem. Rev.* 181 (1999) 147; (b) A.G. Smith, P.A. Tasker, D.J. White, *Coord. Chem. Rev.* 241 (2003) 61; (c) P. Chaudhuri, *Coord. Chem. Rev.* 243 (2003) 143.
- [13] C.J. Milios, Th.C. Stamatatos, S.P. Perlepes, *Polyhedron* 25 (2006) 134 (Polyhedron Report).
- [14] H. Miyasaka, R. Clérac, K. Mizushima, K. Sugiura, M. Yamashita, W. Wernsdorfer, C. Coulon, *Inorg. Chem.* 42 (2003) 8203.
- [15] (a) M.W. Wemple, H.-L. Tsai, S. Wang, J.P. Claude, W.E. Streib, J.C. Huffman, D.N. Hendrickson, G. Christou, *Inorg. Chem.* 35 (1996) 6437; (b) J.B. Vincent, K. Folting, J.C. Huffman, G. Christou, *Inorg. Chem.* 25 (1986) 996.
- [16] J.B. Vincent, H.-R. Chang, K. Folting, J.C. Huffman, G. Christou, D.N. Hendrickson, *J. Am. Chem. Soc.* 109 (1987) 5703.
- [17] (a) G.M. Sheldrick, SHELXS-97, Program for Crystal Structure Solution, University of Göttingen, Germany, 1997; (b) G.M. Sheldrick, SHELXS-97, Program for the Refinement of Crystal Structures from Diffraction Data, University of Göttingen, Germany, 1997; (c) Rigaku/MS, CRYSTALCLEAR, The Woodlands, Texas, USA, 2008.
- [18] (a) H.-L. Tsai, S. Wang, K. Folting, W.E. Streib, D.N. Hendrickson, G. Christou, *J. Am. Chem. Soc.* 117 (1995) 2503; (b) R.C. Squire, S.M.J. Aubin, K. Folting, W.E. Streib, G. Christou, D.N. Hendrickson, *Inorg. Chem.* 34 (1995) 6463.
- [19] N.C. Harden, M.A. Bolcar, W. Wernsdorfer, K.A. Abboud, W.E. Streib, G. Christou, *Inorg. Chem.* 42 (2003) 7067.
- [20] M.A. Halcrow, W.E. Streib, K. Folting, G. Christou, *Acta Crystallogr. C* 51 (1995) 1263.
- [21] K.W. Nordquest, D.W. Phelps, W.F. Little, D.J. Hodgson, *J. Am. Chem. Soc.* 98 (1976) 1104.
- [22] I. Chadjistamatis, A. Terzis, C.P. Raptopoulou, S.P. Perlepes, *Inorg. Chem. Commun.* 6 (2003) 1365.
- [23] R.D. Cannon, R.P. White, *Prog. Inorg. Chem.* 36 (1988) 195.
- [24] C. Papatriantafyllopoulou, C.G. Efthymiou, C.P. Raptopoulou, A. Terzis, E. Manessi-Zoupa, S.P. Perlepes, *Spectrochim. Acta, Part A* 70 (2008) 718.
- [25] G.B. Deacon, R.J. Phillips, *Coord. Chem. Rev.* 33 (1980) 227.
- [26] (a) I.D. Brown, D. Altermatt, *Acta Crystallogr., Sect. B* 41 (1985) 244; (b) W. Liu, H.H. Thorp, *Inorg. Chem.* 32 (1993) 4102.
- [27] H.J. Eppley, S.M.J. Aubin, W.E. Streib, J.C. Bollinger, D.N. Hendrickson, G. Christou, *Inorg. Chem.* 36 (1997) 109.
- [28] A.G. Blackman, J.C. Huffman, E.B. Lobkovsky, G. Christou, *Polyhedron* 11 (1992) 251.
- [29] Th.C. Stamatatos, D. Foguet-Albiol, S.P. Perlepes, C.P. Raptopoulou, A. Terzis, C.S. Patrickios, G. Christou, A.J. Tasiopoulos, *Polyhedron* 25 (2006) 1737, and references cited therein.
- [30] J.B. Vincent, C. Christmas, H.-R. Chang, Q. Li, P.D.W. Boyd, J.C. Huffman, D.N. Hendrickson, G. Christou, *J. Am. Chem. Soc.* 111 (1989) 2086.
- [31] (a) For example see: R.W. Saalfrank, N. Löw, B. Demleitner, D. Stalke, M. Teichert, *Chem. Eur. J.* 4 (1998) 1305; (b) R.W. Saalfrank, N. Löw, S. Trummer, G.M. Sheldrick, M. Teichert, D. Stalke, *Eur. J. Inorg. Chem.* (1998) 559.
- [32] (a) Th.C. Stamatatos, K.A. Abboud, G. Christou, *J. Mol. Struct.*, in press. Available from: <<http://dx.doi.org/10.1016/j.molstruc.2008.04.031>>; (b) C. Boskovic, W. Wernsdorfer, K. Folting, J.C. Huffman, D.N. Hendrickson, G. Christou, *Inorg. Chem.* 41 (2002) 5107; (c) C. Boskovic, J.C. Huffman, G. Christou, *Chem. Commun.* (2002) 2502.
- [33] (a) C.J. Milios, F.P.A. Fabbiani, S. Parsons, M. Murugesu, G. Christou, E.K. Brechin, *Dalton Trans.* (2006) 351; (b) M. Murugesu, W. Wernsdorfer, K.A. Abboud, G. Christou, *Angew. Chem., Int. Ed.* 44 (2005) 892; (c) M. Manoli, C.J. Milios, A. Mishra, G. Christou, E.K. Brechin, *Polyhedron* 26 (2007) 1923.
- [34] (a) R. Bagai, K.A. Abboud, G. Christou, *Inorg. Chem.* 47 (2008) 621; (b) E.K. Brechin, G. Christou, M. Soler, M. Helliwell, S.J. Teat, *Dalton Trans.* (2003) 513; (c) C.J. Milios, R. Inglis, A. Vinslava, A. Prescimone, S. Parsons, S.P. Perlepes, G. Christou, E.K. Brechin, *Chem. Commun.* (2007) 2738.
- [35] (a) For example see: S. Tanase, G. Aromi, E. Bouwman, H. Kooijman, A.L. Spek, J. Reedijk, *Chem. Commun.* (2003) 3147; (b) E.K. Brechin, M. Soler, G. Christou, M. Helliwell, S.J. Teat, W. Wernsdorfer, *Chem. Commun.* (2003) 1276; (c) V.A. Grillo, M.J. Knapp, J.C. Bollinger, D.N. Hendrickson, G. Christou, *Angew. Chem., Int. Ed.* 35 (1996) 1818; (d) H.-L. Tsai, W. Wang, K. Folting, W.E. Streib, D.N. Hendrickson, G. Christou, *J. Am. Chem. Soc.* 117 (1995) 2503; (e) S. Wang, H.-L. Tsai, K. Folting, J.D. Martin, D.N. Hendrickson, G. Christou, *J. Chem. Soc., Chem. Commun.* (1997) 671; (f) E. Libby, K. Folting, J.C. Huffman, G. Christou, *Inorg. Chem.* 32 (1993) 2549; (g) L.F. Jones, E.K. Brechin, D. Collison, J. Raftery, S.J. Teat, *Inorg. Chem.* 42 (2003) 6971.
- [36] A.J. Tasiopoulos, K.A. Abboud, G. Christou, *Chem. Commun.* (2003) 580.
- [37] E.C. Sañudo, V.A. Grillo, M.J. Knapp, J.C. Bollinger, J.C. Huffman, D.N. Hendrickson, G. Christou, *Inorg. Chem.* 41 (2002) 2441, and references cited therein.
- [38] (a) E. Libby, J.K. McCusker, E.A. Schmitt, K. Folting, D.N. Hendrickson, G. Christou, *Inorg. Chem.* 30 (1991) 3486; (b) S. Wang, K. Folting, W.E. Streib, E.A. Schmitt, J.K. McCusker, D.N. Hendrickson, G. Christou, *Angew. Chem., Int. Ed.* 30 (1991) 305; (c) G. Aromi, S. Bhaduri, P. Artus, J.C. Huffman, D.N. Hendrickson, G. Christou, *Polyhedron* 21 (2002) 1799; (d) C. Cañada-Vilalta, J.C. Huffman, G. Christou, *Polyhedron* 20 (2001) 1785.
- [39] C. Papatriantafyllopoulou, C.P. Raptopoulou, A. Terzis, J.F. Janssens, S.P. Perlepes, E. Manessi-Zoupa, *Z. Naturforsch.* 62b (2007) 1123.